Mechanical Properties of ASTM A992 Steel After Fire

JINWOO LEE, MICHAEL D. ENGELHARDT and ERIC M. TALEFF

ABSTRACT

When evaluating the condition and safety of a steel structure following a fire, an issue of concern is the mechanical properties of the steel after the fire. The exposure of the steel to high temperatures during the fire, and the subsequent cooling of the steel after the fire, can potentially affect the mechanical properties of the steel. A testing program was undertaken to measure the mechanical properties of ASTM A992 steel after being subjected to various patterns of heating and cooling. This paper presents results of the test program and provides data on the effect of various heating and cooling cycles on key mechanical properties, including yield strength, tensile strength, elastic modulus, elongation, Charpy V-Notch (CVN) impact values and hardness.

Keywords: fire, mechanical properties, steel, ASTM A992.

INTRODUCTION

When a structure has been exposed to fire, an issue of concern following the fire is evaluating the safety of the structure and the need for repairs (Gosain et al., 2008; Tide, 1998). In the case of a steel structure, questions arise on the effect that the exposure to heating and cooling may have had on the mechanical properties of the structural steel. Limited past studies have addressed the post-fire mechanical properties of structural steel (Smith et al., 1981; Outinen and Makelainen, 2004), whereas other studies have examined the effects of various cooling rates from a more fundamental metallurgical and microstructure point of view (Davis and King, 1993; Dhua et al., 2003; Pyshmintsev et al., 2008). However, the available experimental data pertinent to post-fire evaluation of structural steel are limited. Further, a review of the literature suggests there are no data available on the effects of heating and cooling on the mechanical properties of ASTM A992 steel, which is currently the most common structural steel used for rolled wide flange shapes in the United States. To address the need for such data, the authors conducted an extensive series of tests on A992 steel to help engineers assess the post-fire mechanical properties of this material. More complete details of this investigation will be reported in an upcoming publication by Lee (2012).

Jinwoo Lee, P.E., Ph.D. candidate, Department of Civil, Architectural and Environmental Engineering, University of Texas at Austin, Austin, TX. E-mail: jinwoo@mail.utexas.edu

Michael D. Engelhardt, Ph.D., P.E., Dewitt C. Greer Centennial Professor, Department of Civil, Architectural and Environmental Engineering, University of Texas at Austin, Austin, TX (corresponding author). E-mail: mde@mail.utexas.edu

Eric M. Taleff, Ph.D., Professor, Department of Mechanical Engineering, University of Texas at Austin, Austin, TX. E-mail: taleff@mail.utexas.edu

TEST PROGRAM

Material Samples

For the purposes of this study, a series of coupons were prepared as shown in Figure 1. The coupons were made from material taken from the web of a W30×99 shape of ASTM A992 steel. The longitudinal dimension of the coupon corresponded with the longitudinal axis of the member, i.e., along the rolling direction. Room temperature tension tests on this material prior to heating and cooling showed F_y = 52 ksi for yield strength and F_u = 66 ksi for tensile strength. The results of a chemical analysis of the steel are shown in Table 1. Two different lengths of coupons were made for testing; 14 in. and 18 in. The longer coupons were used to extract samples for Charpy V-Notch testing.

Heating

The coupons were heated in an ATS (Applied Test Systems) 3160 electric furnace. The basic heating system is shown in Figure 2, including the furnace, the furnace controller, and the data acquisition system for recording temperatures. The coupons were hung from the top of the furnace using wire and were thus surrounded by air on all sides. The temperature of the coupons was measured using K-type thermocouple wire. The thermocouple wire was wrapped around the center portion of the coupon and covered with stainless steel foil to minimize radiation effects of the furnace heating coils on the thermocouple. Most of coupons were heated up to the target temperature within a half-hour and then held at that target temperature for one hour. Coupons were heated to target temperatures that ranged from 200 to 1,000 °C, in increments of 100 °C. In this paper, all temperatures are reported in the Celsius scale (t°F = 1.8 × t°C + 32).

Table 1. Chemical Composition of the Test Material											
Element	C	Si	Mn	P	S	Cr	Mo	Ni	V	Al	Cu
Weight (%)	0.079	0.20	0.97	0.014	0.024	0.09	0.026	0.13	0.027	0.001	0.38

Cooling

The actual cooling rates for structural steel after a fire can depend on a number of factors, including the cooling rate of the fire itself, whether or not the steel is insulated, whether or not the steel is exposed to water from fire-fighting operations or sprinklers, and others. Three different cooling methods were used for the test coupons in an attempt to provide a range of cooling rates that might reasonably bracket realistic conditions. The three cooling methods are referred to as cooled-in-blanket (CIB), cooled-in-air (CIA) and cooled-in-water (CIW). Figure 3 shows photos of coupons being cooled by these methods. The CIB method provided the slowest cooling. For this method, the coupon was wrapped in a ceramic fiber blanket after removal from the furnace and allowed to cool to room temperature. For the CIA method, the coupon was removed from the furnace and allowed to cool to room temperature while exposed to ambient air. For the CIW method, the coupon was removed from the furnace and placed in a container of water for very rapid cooling. The time required for the coupons at 1,000 °C to return to room temperature was on the order of 14 hours for CIB, 4 hours for CIA and 1 minute for CIW. The actual cooling rates were monitored for each coupon. Typical cooling data are shown in Figure 4. Figure 4a plots temperature versus time for both the heating and cooling of the coupons heated to 1,000 °C. All three cooling methods are shown in the plot. Figure 4b shows the cooling rate (in °C/min) for coupons heated to various temperatures and then cooled by the CIB method. The actual cooling rate varied over time for each cooling method. An example of cooling rates measured 1-minute after removal of the coupon from the furnace for the CIA and CIB methods is given in Table 2.

Cleaning

After the heating and cooling process, a number of the coupons had a significant amount of scale and corrosion. To

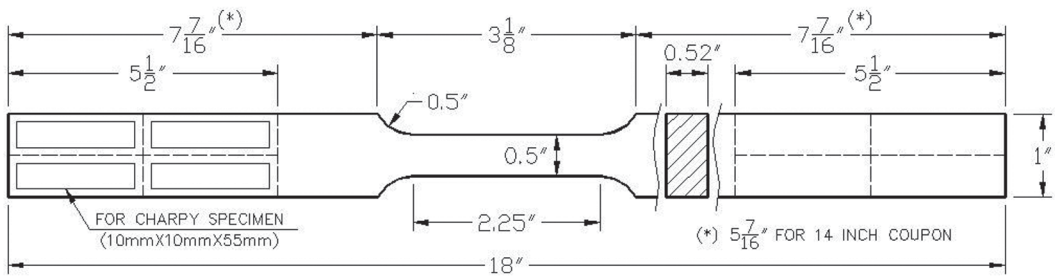

Fig. 1. Coupon dimensions.

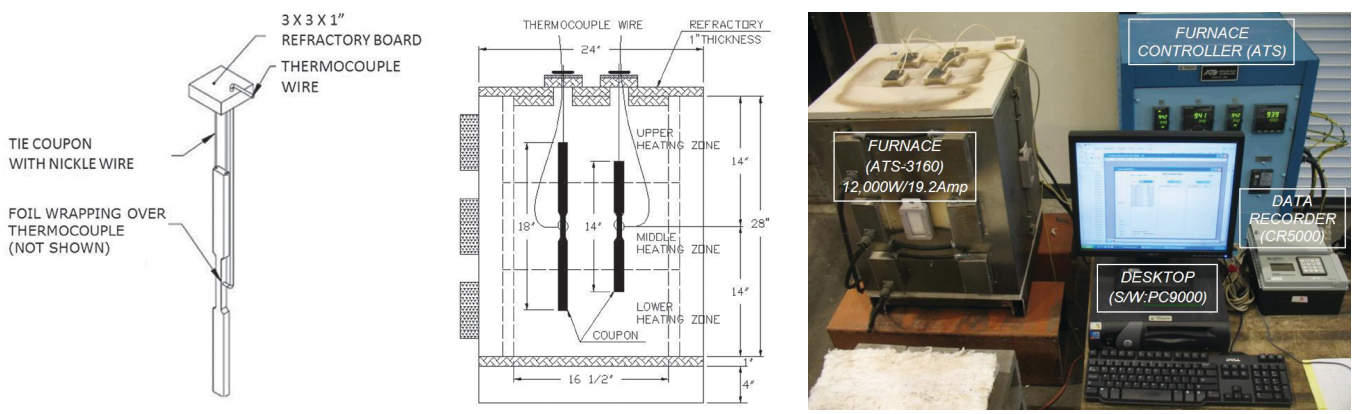

Fig. 2. Coupon heating system.

Table 2. Measured Cooling Rates 1-Minute After Removal from Furnace										
Temp (°C)	CIA (°C/Min)					CIB (°C/Min)				
	0~30	60	90	120	180	0~30	60	90	120	180
200	4.48	0.97	0.32	0.13	0.04	1.89	0.93	0.70	0.56	0.41
300	7.26	1.46	0.36	0.14	0.05	3.21	1.30	0.99	0.77	0.55
400	10.49	1.61	0.39	0.09	0.01	4.57	1.95	1.43	1.07	0.71
500	13.32	1.88	0.55	0.19	0.05	6.08	2.44	1.77	1.30	0.87
600	16.87	1.83	0.37	0.1	0.02	7.79	3.51	2.25	1.50	0.84
700	19.28	2.27	0.64	0.23	0.07	9.77	4.21	2.58	1.69	1.00
800	22.62	2.27	0.62	0.18	0.04	9.73	4.85	3.15	2.09	1.27
900	25.05	2.95	0.75	0.23	0.06	11.21	5.14	3.45	2.34	1.44
1,000	28.97	2.52	0.70	0.24	0.06	13.22	5.17	3.52	2.49	1.57

Fig. 3. Cooled-in-air (CIA), cooled-in-blanket (CIB) and cooled-in-water (CIW).

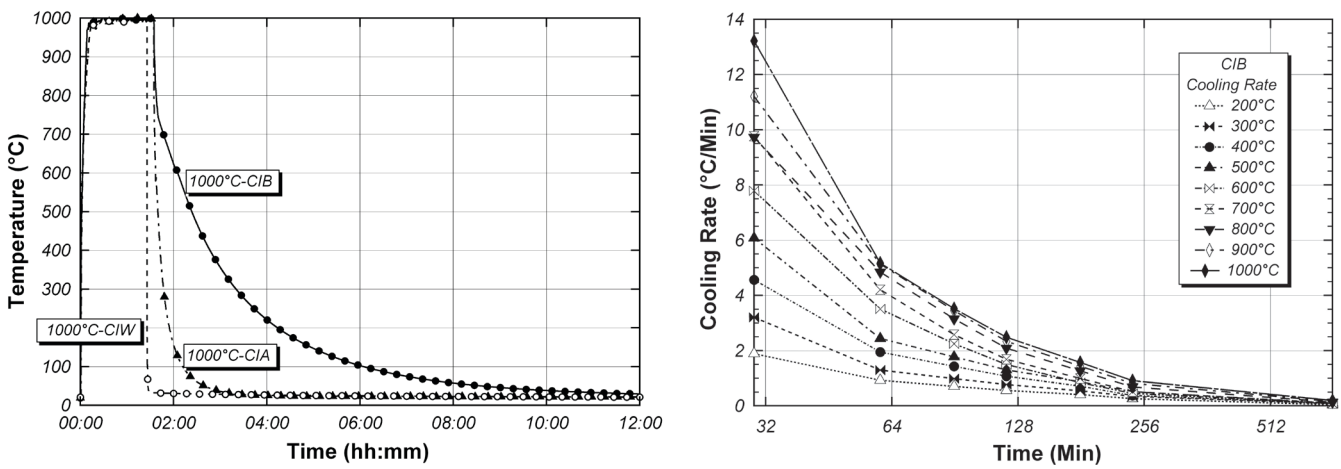

(a) Temperature vs. Time for 1,000 °C coupons

(b) Cooling Rate vs. Time for CIB coupons

Fig. 4. Typical temperature data.

allow for accurate measurement of cross-section area and for secure attachment of the extensometer, the coupons were cleaned with a wire brush grinder prior to testing. Figure 5 shows photos of typical coupons before and after cleaning.

Testing

After heating, cooling and cleaning, tensile tests were performed on the coupons using an MTS 810, 22-kip capacity, computer-controlled, test machine. Coupons were loaded with displacement control at a cross-head rate of 0.01 in. per minute. The strain was measured with a 2-in. gage length MTS extensometer. Charpy V-Notch tests as well as hardness tests were also conducted.

TEST RESULTS

Stress-Strain Curves

Figures 6 through 11 show the measured stress strain curves for all coupons for each type of cooling. The temperatures shown in these plots indicate the temperature to which the coupon was heated (and held for 1-hour) prior to cooling. The full stress-strain curves are shown as well as the initial portion of the curves up to 1% strain. Each plot also shows the virgin stress-strain curve at 20 °C, which was for the coupon not subjected to heating and cooling. The full stress-strain curves are replotted in Figures 12 through 20 according to the heating temperature of the coupon. The virgin stress-strain curve for unheated steel is again also plotted for comparison. Note that for the CIA and CIB cooling methods, the coupons were heated to temperatures varying from 200 to 1,000 °C in increments of 100 °C. For the CIW cooling method, the coupons were heated to temperatures varying from 500 to 1,000 °C in increments of 100 °C. These data show that for heating temperatures up to about 500 °C, the stress-strain curves for the heated and cooled coupons are very similar to the virgin unheated coupon for all cooling methods. However, for heating temperatures of 600° C and above, some changes from the virgin coupon become somewhat more noticeable. For the heating range of 600 to 1,000 °C, the CIA and CIB coupons show some reduction in yield and tensile strength. The stress-strain curves, however,

Fig. 5. Coupons before and after cleaning.

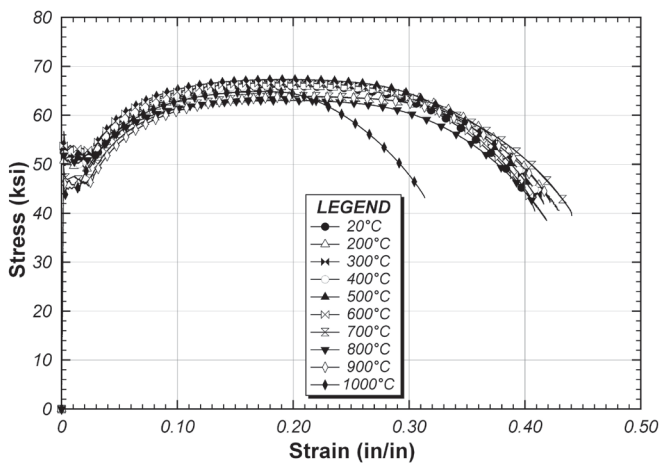

Fig. 6. CIA full stress-strain curves.

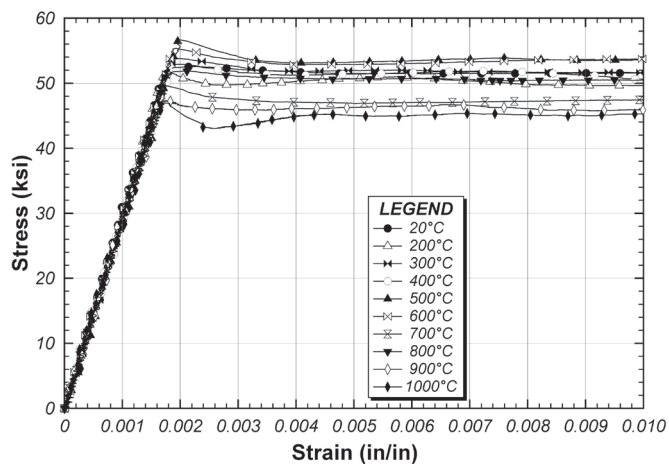

Fig. 7. CIA initial portion of stress-strain curves.

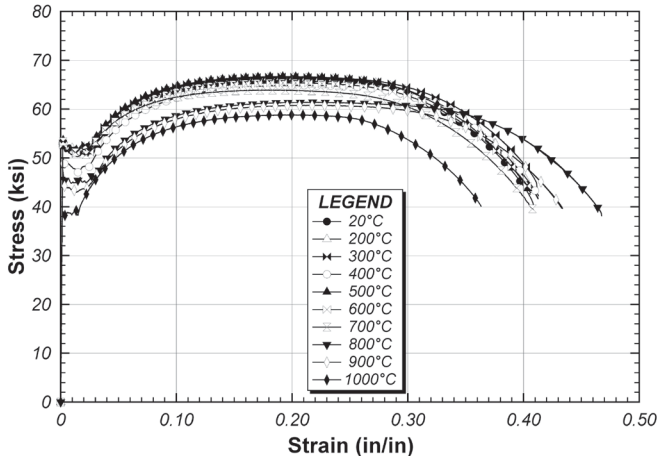

Fig. 8. CIB full stress-strain curves.

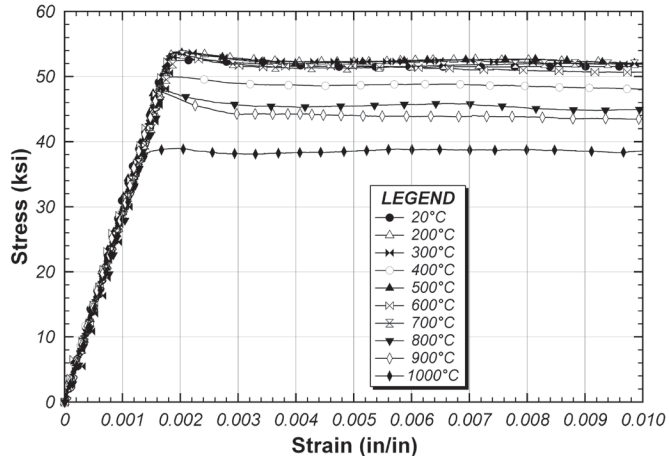

Fig. 9. CIB initial portion of stress-strain curves.

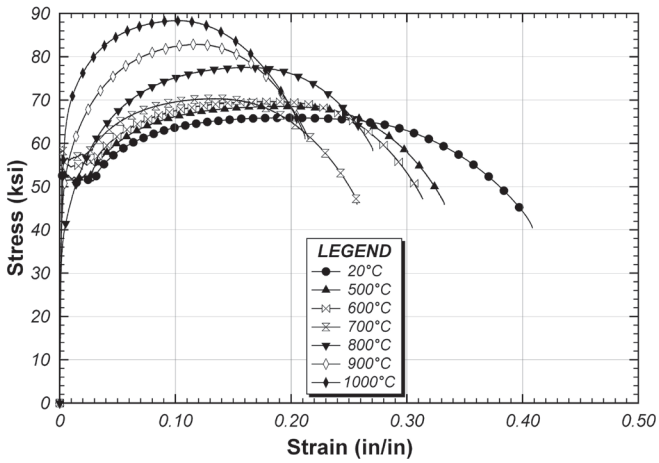

Fig. 10. CIW full stress-strain curves.

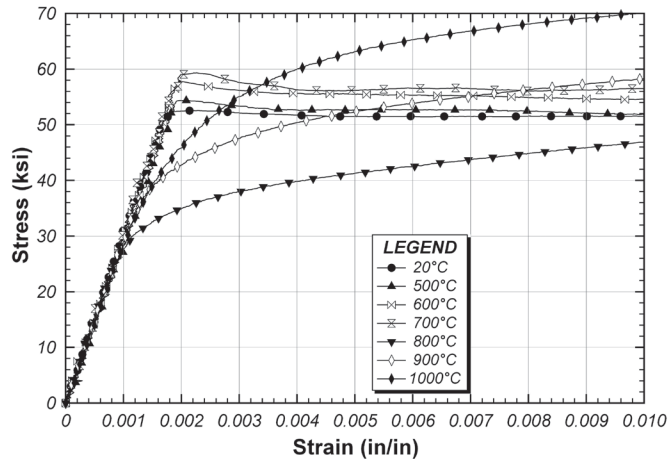

Fig. 11. CIW initial portion of stress-strain curves.

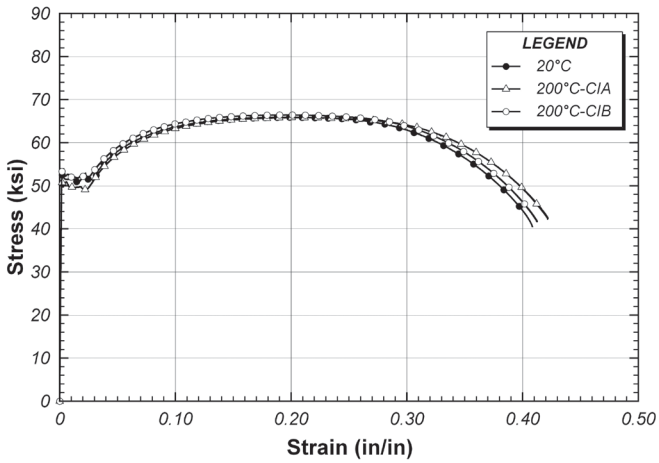

Fig. 12. Stress-strain curves for 200 °C.

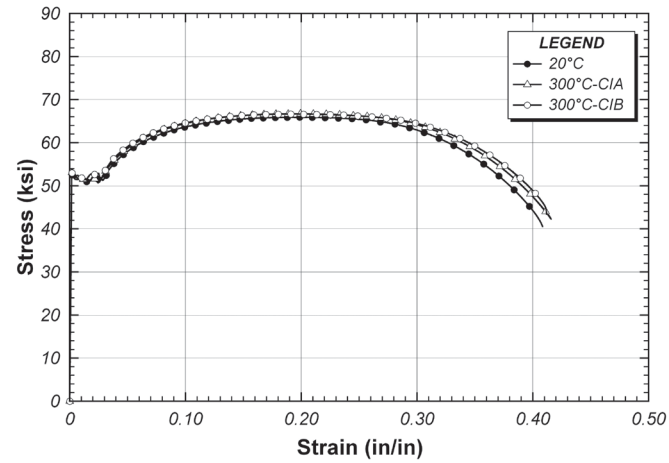

Fig. 13. Stress-strain curves for 300 °C.

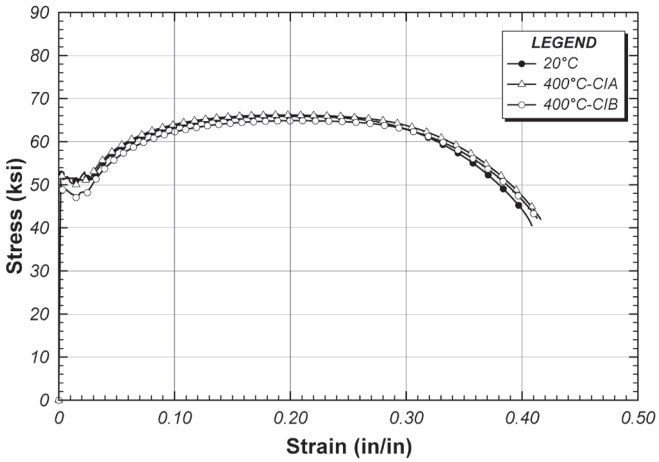

Fig. 14. Stress-strain curves for 400 °C.

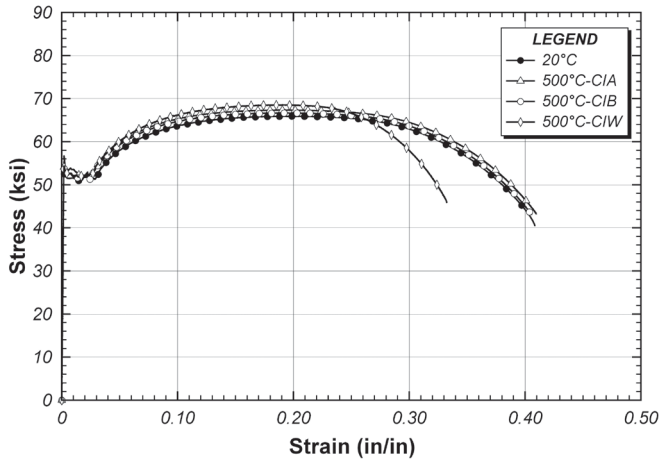

Fig. 15. Stress-strain curves for 500 °C.

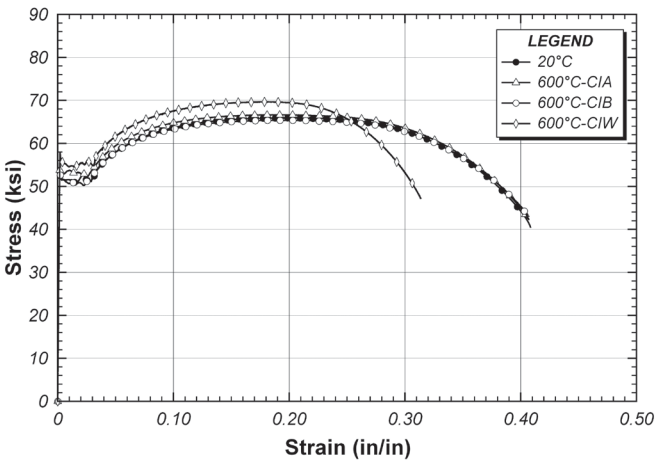

Fig. 16. Stress-strain curves for 600 °C.

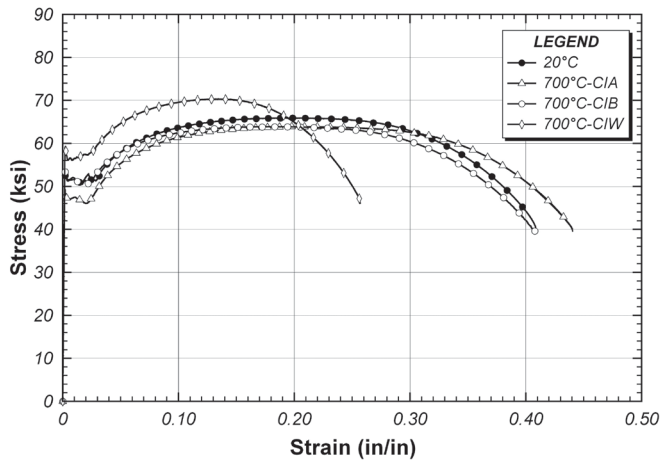

Fig. 17. Stress-strain curves for 700 °C.

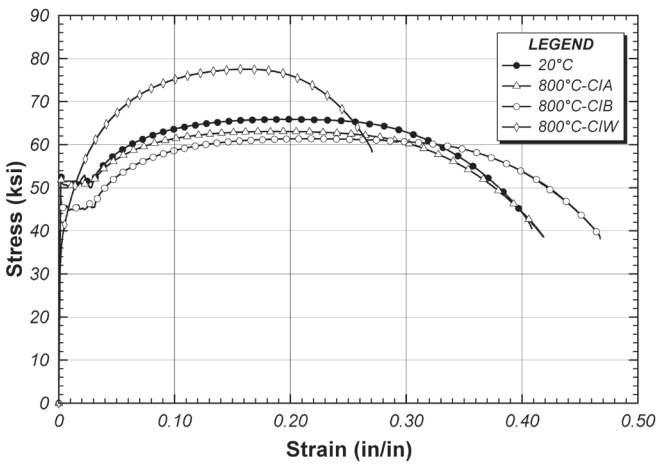

Fig. 18. Stress-strain curves for 800 °C.

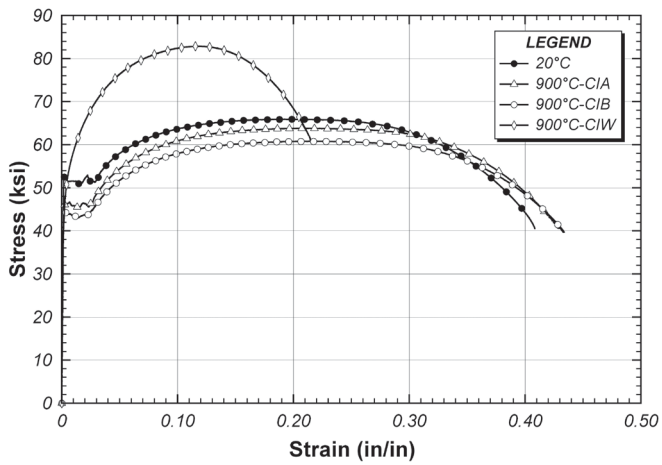

Fig. 19. Stress-strain curves for 900 °C.

Table 3. Yield Strength (ksi)										
Temp. (°C)	20	200	300	400	500	600	700	800	900	1,000
CIA	51.9	50.1	52.1	51.3	53.1	52.9	50.8	47.1	46.0	44.6
CIB	51.9	52.4	52.3	48.7	52.2	51.6	51.4	45.4	44.3	38.3
CIW	51.9	—	—	—	52.7	55.6	56.6	38.7	49.4	60.1

maintain the same basic shape of the virgin curve, exhibiting a well-defined yield plateau. Within the 600 to 1,000 °C heating range, more significant changes are evident in the CIW coupons. Compared to the virgin coupon, the CIW coupons exhibit a significant increase in tensile strength and a significant loss of ductility. For heating temperatures in the range of 800 to 1,000 °C, the CIW stress-strain curves do not exhibit a yield plateau and show significant nonlinearity starting at relatively low stress levels. In general, more significant changes in the stress-strain curves are expected for coupons heated in the range of 800 to 1,000 °C, because steel undergoes a phase change near 730 °C from ferrite (α-Fe) to austenite (γ-Fe).

Yield Strength

The yield strength of the coupons after heating and cooling was determined from the stress-strain curves by using the 0.2% offset method shown on Figure 21. Results are listed in Table 3 and are plotted in Figure 22. The right plot in

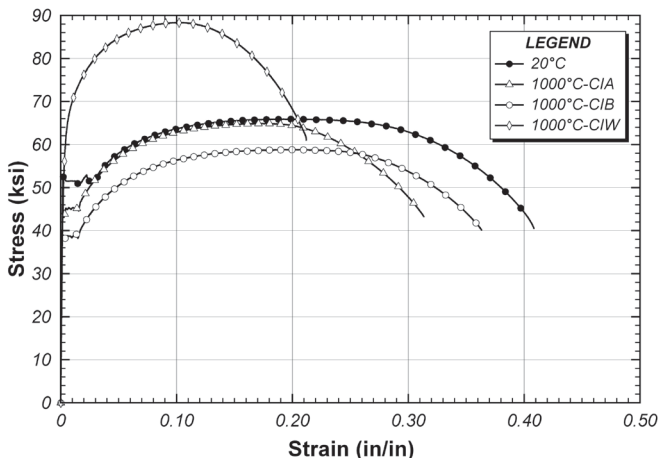

Fig. 20. Stress-strain curves for 1,000 °C.

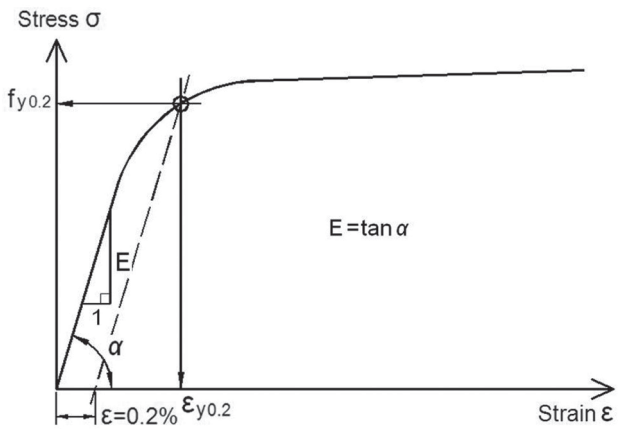

Fig. 21. Definition of 0.2% offset yield stress.

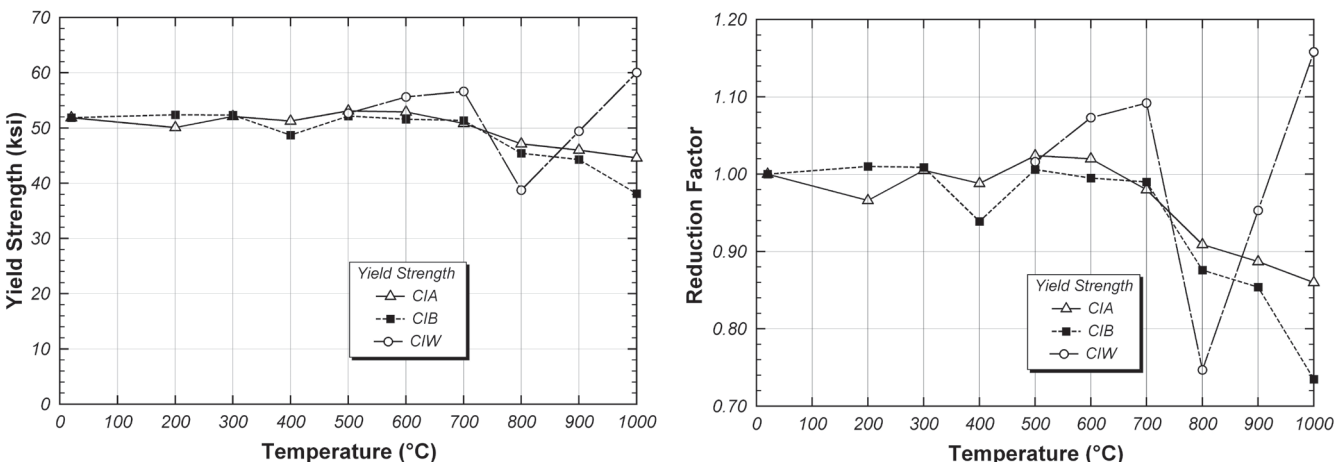

Fig. 22. Yield strength and yield strength reduction factors after heating and cooling.

Table 4. Tensile Strength (ksi)										
Temp. (°C)	20	200	300	400	500	600	700	800	900	1,000
CIA	65.9	65.9	66.8	66.2	67.4	66.7	63.1	63.9	63.8	64.9
CIB	65.9	66.5	66.7	64.9	66.7	65.4	63.9	61.5	60.8	58.8
CIW	65.9	—	—	—	68.6	69.7	70.4	77.6	82.9	88.4

Figure 22 shows the reduction in yield strength relative to the virgin unheated coupon. Reasonably significant reductions in yield strength, up to about 25% for CIA and CIB cooling are seen for coupons heated to temperatures of 800 to 1,000 °C. The CIW coupons also show significant changes in yield strength in the range of 800 to 1,000 °C, with the yield strength first dropping and then increasing within this temperature range.

Specimens heated to temperatures higher than 727 °C at least partially transform to austenite (γ-Fe), and subsequent cooling can produce microstructures different from the original material. This is one reason that yield strength does not change significantly in specimens heated to 700 °C and lower temperatures. The decrease in yield strength with increase in temperature at 800 °C and higher in the CIB and CIA specimens results from increasing volume fractions transformed to austenite during heating. Upon subsequent cooling, the ferrite (α-Fe) produced may be coarser than that of the original material, leading to decreased yield strength. A992 steel has sufficient carbon to potentially form some pearlite following cooling from these temperatures. Pearlite consists of ferrite (α-Fe) and cememtite (Fe_3C) in a lamellar configuration. The amount of pearlite possible increases with the amount of austenite transformed during heating, which should increase from 727 °C up to a maximum near 900 °C. The microstructures expected after cooling from 800 °C or higher are a normalized microstructure with some coarse pearlite for slow cooling rates (e.g., CIB) and some slightly finer pearlite for moderate cooling rates (e.g., CIA). This may explain the slightly greater yield strength reduction observed for the CIB specimens compared to the CIA specimens. An increase in cooling rate (e.g., CIW) will reduce the pearlite interlamellar spacing and, in accordance with the continuous cooling transformation curve, will lead to an increase in yield strength, such as that observed for the CIW specimen heated at 1,000 °C. Thus, the variations of yield strength with heating temperature and cooling rate, as seen in Figure 22, are consistent with the expected microstructural transformations.

Tensile Strength

The tensile strength of the coupons after heating and cooling was determined from the stress-strain curves. Results are listed in Table 4 and are plotted in Figure 23. For the CIA and CIB cooling methods, there is a modest reduction in tensile strength for coupons heated above about 600 °C. On the other hand, for the CIW cooling method, there is a large increase in tensile strength for coupons heated above about 600 °C due to quenching effect, which induced a martensite microstructure of metal with quick cooling process. A transformed martensite generally represents strength increasing

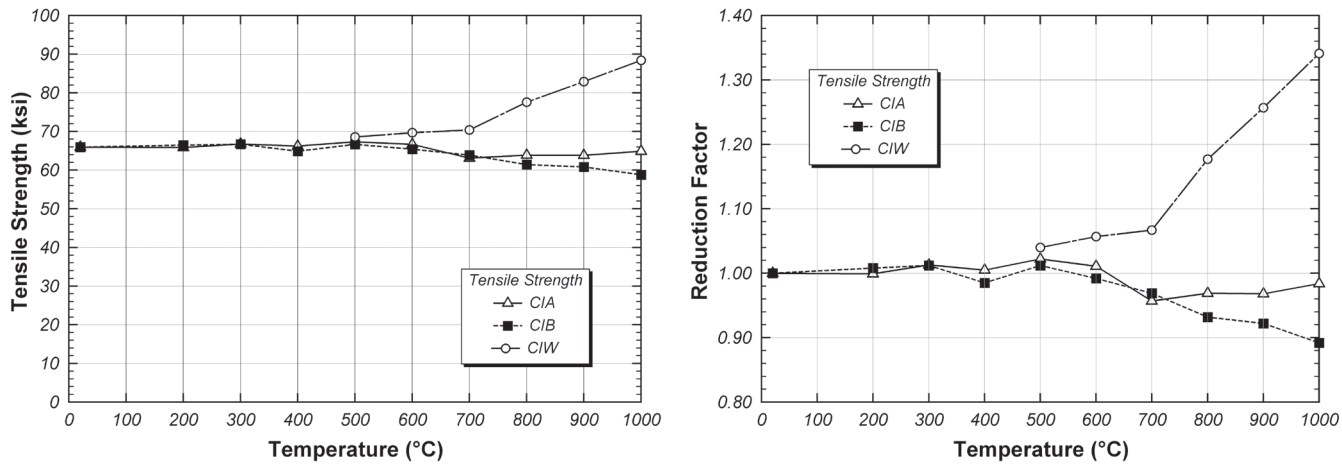

Fig. 23. Tensile strength and tensile strength reduction factors after heating and cooling.

Table 5. Elastic Modulus (ksi)										
Temp. (°C)	20	200	300	400	500	600	700	800	900	1,000
CIA	29,910	29,900	29,420	28,780	28,930	29,510	29,040	28,830	29,010	28,200
CIB	29,910	28,720	29,270	29,360	29,590	28,800	28,060	28,080	29,680	27,610
CIW	29,910	—	—	—	29,090	29,690	30,380	29,380	29,520	28,650

and ductility decreasing trend because of trapped austenite microstructures produced by rapid cooling period.

Elastic Modulus

The elastic modulus of the coupons after heating and cooling was estimated from the initial linear portion of the stress-strain curves. Strains were measured in the tension coupon tests using a nonaveraging type extensometer; i.e. strains were measured on only one side of the coupon. Consequently, errors at small strain levels can occur due to bending of the coupon, resulting in errors in the measured strain. As such, the elastic modulus values derived from the stress-strain curves may be subject to some error. Nonetheless, the elastic modulus data were still examined for general trends. Results are listed in Table 5 and are plotted in Figure 24. The data show minor variations in elastic modulus over the full temperature range. These variations may be indicative of strain measurement errors and so the data are considered somewhat inconclusive. Note, however, that even considering possible strain measurement errors, the data show no dramatic changes in elastic modulus.

Elongation

The elongation of the coupons after heating and cooling was determined from the stress-strain curves. The elongation was taken as the strain at fracture of the coupon. Results are listed in Table 6 and are plotted in Figure 25. For the CIA and CIB cooling methods, there is no significant change in elongation for temperatures up to 900 °C. There is a reduction in the measured elongation for the coupons heated to 1,000 °C. Even for this case, however, the elongation was still above 30%. The CIW coupons, on the other hand, show a rather significant reduction in elongation over the 500 to 1,000 °C range of temperatures tested.

Charpy V-Notch (CVN) Impact Tests

Charpy V-Notch impact tests were conducted on samples of steel that were subjected to heating and cooling. Results are listed in Table 7 and are plotted in Figure 26. The results for the CIA and CIB specimens show an increase in CVN values over the full temperature range tested. The CIW specimens, on the other hand, show a large reduction in CVN values for the temperature range tested, which was 500 to 1,000 °C. Note that specimens heated to 1,000 °C and then cooled in water showed a CVN value that was only 20% of the original virgin specimen.

Hardness Tests

Hardness tests were conducted on samples of steel subjected to heating and cooling. An objective of these tests was to

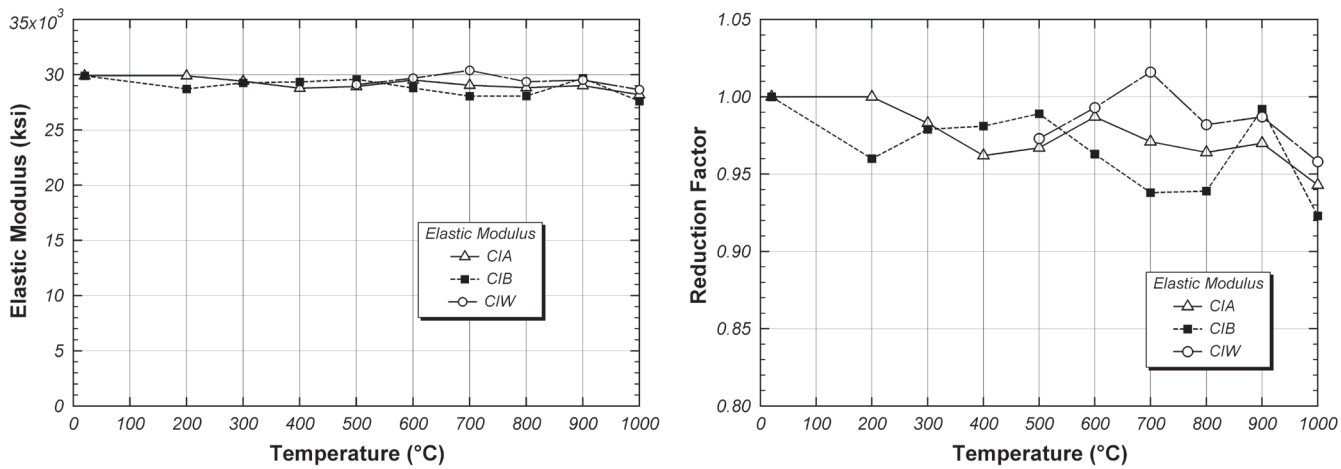

Fig. 24. Elastic modulus and elastic modulus reduction factors after heating and cooling.

Table 6. Elongation										
Temp. (°C)	20	200	300	400	500	600	700	800	900	1,000
CIA	0.41	0.42	0.42	0.42	0.41	0.41	0.44	0.42	0.43	0.31
CIB	0.41	0.41	0.41	0.41	0.41	0.41	0.41	0.47	0.43	0.36
CIW	0.41	—	—	—	0.33	0.32	0.26	0.27	0.21	0.21

determine if hardness testing can be used as a diagnostic tool to evaluate steel after exposure to fire. Hardness measurements were made using a Wilson Rockwell Hardness Tester. All hardness results were within the B scale range except for the 1,000 °C CIW coupon, which was in the C scale Rockwell hardness range. The measured hardness values are plotted in Figure 27 and are listed in Table 8. The trends in Rockwell hardness with heating temperature and cooling method are very similar to the corresponding trends in tensile strength (Figure 23). This is expected because there is typically a strong correlation between hardness and tensile strength. On the other hand, the correlation between hardness (Figure 27) and yield strength (Figure 22) is rather poor. Consequently, when evaluating steel after a fire, hardness testing may not be effective in diagnosing loss of yield strength. Hardness testing, on the other hand, may be useful for diagnosing steel that has been exposed to high temperatures and then rapidly cooled by water.

CONCLUSIONS

This paper has presented results of tension tests and CVN tests on samples of A992 steel subjected to heating and cooling. These tests were intended to provide insights into the post-fire mechanical properties of A992 steel. The trends in the data can be summarized as follows. In terms of yield strength, there was no significant reduction until the temperature exceeded 700 °C. For temperatures of 800 up to 1,000 °C, some reduction in yield strength was observed. The largest reduction in yield strength observed in these tests was approximately 25%. This occurred for the coupon heated to 1,000 °C and then cooled very slowly (CIB). For tensile strength, there is little change, even for coupons heated to 1,000 °C. It is noted that the CIW case actually increased the tensile strength. The most significant effect of water cooling appears to be in CVN values. Steel samples that were heated above 500 °C and then cooled rapidly in water showed a large drop in CVN values. CVN values are indicative of fracture toughness, and the loss of fracture toughness due to heating and then rapid cooling in water may be of concern in some applications—for example, in a steel bridge girder subjected to fire and then cooled rapidly by water from fire-fighting operations. It may be possible to identify steel in a structure that was subjected to fire and then cooled rapidly by the use of field hardness measurements.

The data presented in this paper can assist in assessing the post-fire condition of a steel structure. However, these data presume that the maximum temperature achieved in the steel during the fire is known. This, of course, is rarely the case. A review of the literature suggests there are no simple and reliable approaches for estimating the maximum temperature achieved in a steel element during a fire. Some approaches

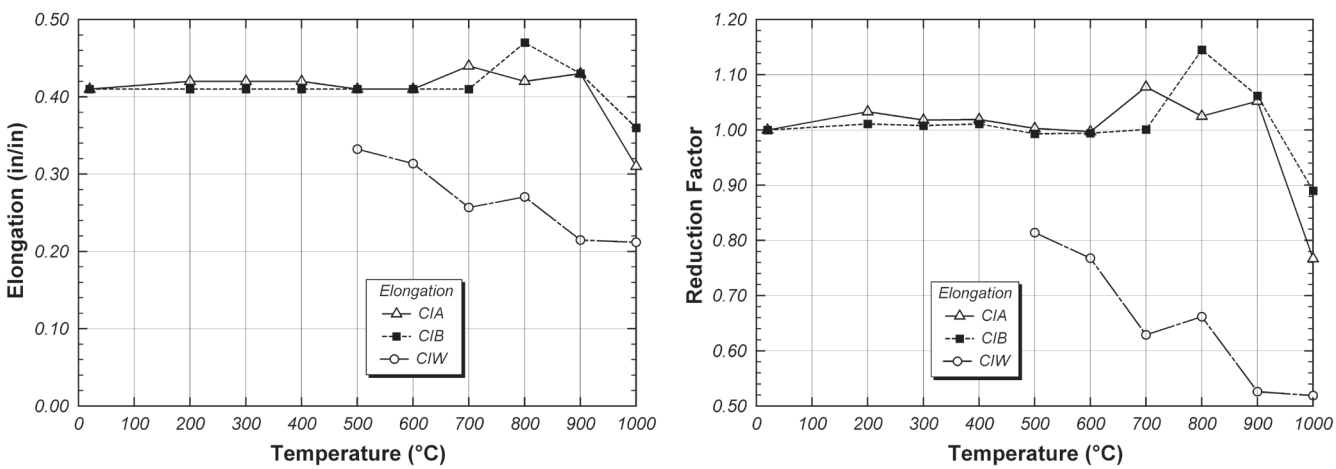

Fig. 25. Elongation and elongation reduction factors after heating and cooling.

Table 7. CVN Impact Energy (ft-lb)										
Temp. (°C)	20	200	300	400	500	600	700	800	900	1,000
CIA	171	220	244	244	240	206	247	245	252	188
CIB	171	233	238	226	219	250	247	259	251	239
CIW	171	—	—	—	95	93	76	79	86	38

Table 8. Rockwell Hardness Test Results (All B scale except for CIW at 1,000 °C)										
Temp. (°C)	20	200	300	400	500	600	700	800	900	1,000
CIA	89	91	87	83	84	86	83	84	82	88
CIB	89	88	88	89	89	89	86	84	81	84
CIW	89	—	—	—	84	85	88	93	97	25.9 (HRC)

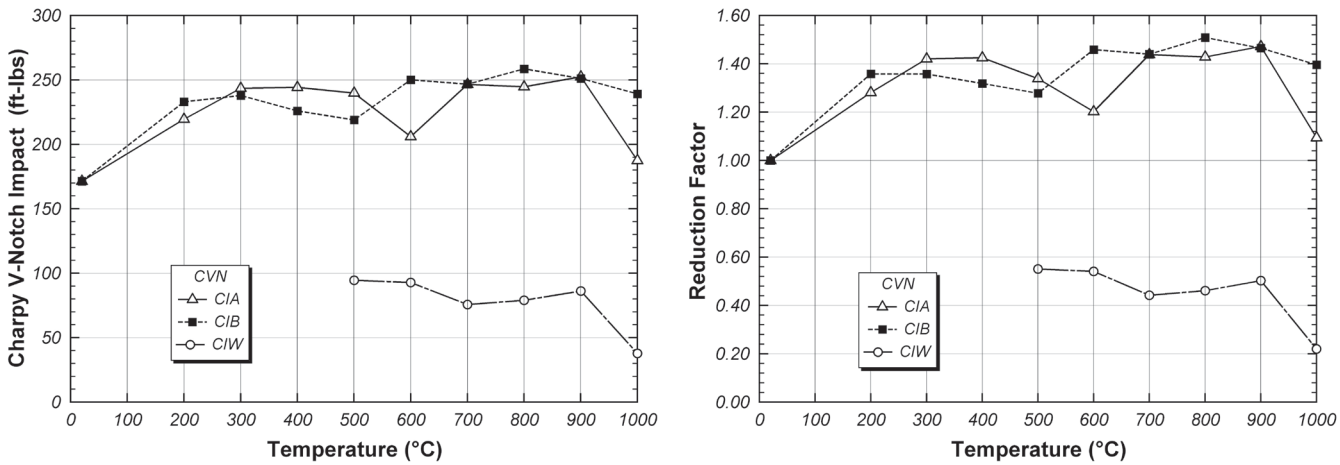

Fig. 26. CVN impact energy and CVN reduction factors after heating and cooling.

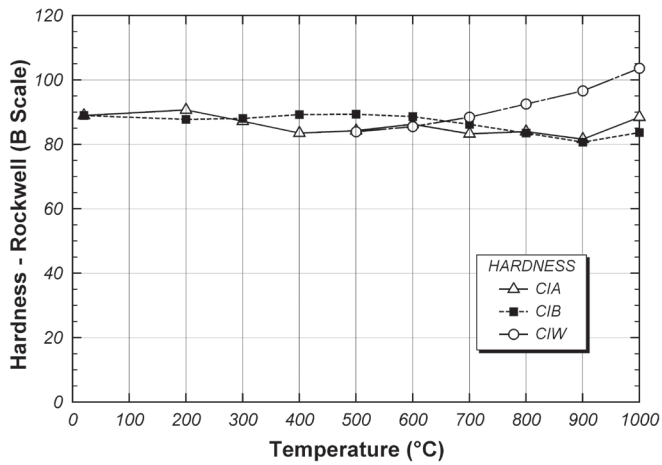

Fig. 27. Rockwell hardness after heat and cooling.

for addressing this question are discussed in Banovic and Foecke (2005). Nonetheless, the tests reported herein examined temperature exposures up to 1,000 °C, which would represent quite an extreme exposure. Even when exposed to such an extreme temperature, there was little degradation in mechanical properties after cooling, with the possible exception of steel cooled rapidly in water. It is important to note, however, that tests on high-strength bolts have shown significant loss of strength after heating and cooling (Yu and Frank, 2009). Thus, when assessing the condition of a steel structure following a fire, the effect of the fire on the strength of bolts is likely to be a greater concern than the effect of the fire on the structural steel members.

ACKNOWLEDGMENTS

The research reported herein was partially supported by the National Science Foundation under Grant No. 0927819. The support of the National Science Foundation and of NSF Program Director M.P. Singh is gratefully acknowledged. Any opinions, findings and conclusions or recommendations expressed in this paper are those of the authors and do not necessarily reflect the views of the National Science Foundation.

REFERENCES

Banovic, S.W. and Foecke, T. (2005), "Federal Building and Fire Safety Investigation of the World Trade Center Disaster: Damage and Failure Modes of Structural Steel Components," Report NIST NCSTAR 1-3C, National Institute of Standards and Technology, Gaithersburg, MD.

Davis, C.L. and King, J.E. (1993), "Effect of Cooling Rate on Intercritically Reheated Microstructure and Toughness in High-Strength Low-Alloy Steel," *Materials Science and Technology,* Vol. 9, No. 1, pp. 8–15.

Dhua, S.K., Mukerjee, D. and Sarma, D.S. (2003), "Effect of Cooling Rate on the As-Quenched Microstructure and Mechanical Properties of HSLA-100 Steel Plates," *Metallurgical and Materials Transactions a-Physical Metallurgy and Materials Science*, Vol. 34A, No. 11, pp. 2493–2504.

Gosain, N.K., Drexler, R.F. and Choudhuri, D. (2008), "Evaluation and Repair of Fire Damaged Buildings," *Structure*, September 2008, pp. 18–22.

Lee, J. (2012), "Elevated Temperature Properties of Steel for Structural Fire Engineering Analysis," Ph.D. Dissertation, Department of Civil, Architectural and Environmental Engineering, University of Texas at Austin (expected completion in 2012).

Outinen, J. and Makelainen, P. (2004), "Mechanical Properties of Structural Steel at Elevated Temperatures and After Cooling Down," *Fire and Materials*, Vol. 28, Nos. 2–4, pp. 237–251.

Panigrahi, B.K. (2006), "Microstructures and Properties of Low-Alloy Fire Resistant Steel," *Bulletin of Materials Science,* Vol. 29, No. 1, pp. 59–66.

Pyshmintsev, I., Boryakova, I.A. and Smirnov, M.A. (2008), "Effect of Cooling Rate on the Structure and Properties of Low-Carbon Tube Steel," *Metallurgist,* Vol. 52, Nos. 7–8, pp. 464–469.

Smith, C.I., Kirby, B.R., Lapwood, D.G., Cole, K.J., Cunningham, A.P. and Preston, R.R. (1981), "The Reinstatement of Fire Damaged Steel Framed Structures," *Fire Safety Journal*, Vol. 4, No. 1, pp. 21–62.

Tide, R.H.R. (1998), "Integrity of Structural Steel After Exposure to Fire," *Engineering Journal*, AISC, Vol. 35, No. 1, pp. 26–38.

Yu, L. and Frank, K.H. (2009), "Shear Behavior of A325 and A490 High-Strength Bolts in Fire and Post-Fire," *Engineering Journal*, AISC, Vol. 46, No. 2, pp. 99–106.